Acta Cryst C STRUCTURAL CHEMISTRY

ISSN 2053-2296

A fluorophore-labelled copper complex: crystal structure, hybrid cyclic water–perchlorate cluster and biological properties

Satish S. Bhat,[a]* Vidyanand K. Revankar,[a]* Naveen Shivalingegowda[b] and N. K. Lokanath[c]

[a]Department of Chemistry, Karnatak University, Pavate Nagar, Dharwad, Karnataka 580 003, India, [b]Institution of Excellence, University of Mysore, Mysuru, Karnataka 570 006, India, and [c]Department of Studies in Physics, University of Mysore, Mysuru, Karnataka 570 006, India. *Correspondence e-mail: bhatsatish111@gmail.com, vkrevankar@rediffmail.com

Received 20 July 2017
Accepted 8 August 2017

Edited by A. L. Spek, Utrecht University, The Netherlands

Keywords: cyclic cluster; fluorophore; copper; crystal structure; water–perchlorate cluster.

CCDC reference: 1562837

Supporting information: this article has supporting information at journals.iucr.org/c

A fluorophore-labelled copper(II) complex, aquabis(dimethylformamide-κO)(perchlorato-κO)[2-(quinolin-2-yl)-1,3-oxazolo[4,5-*f*][1,10]phenanthroline]copper(II) perchlorate monohydrate, $[Cu(ClO_4)(C_{22}H_{12}N_4O)(C_3H_7NO)_2(H_2O)]ClO_4\cdot H_2O$, has been synthesized and characterized. A cyclic hydrogen-bonded water–perchlorate anionic cluster, *i.e.* $[(ClO_4)_2(H_2O)_2]^{2-}$, has been identified within the structure. Each cyclic anionic cluster unit is interconnected by hydrogen bonding to the cation. The cations join into an infinite hydrogen-bonded chain running in the [010] direction. Furthermore, interaction of the complex with calf-thymus DNA (CT-DNA) and cellular localization within the cells was explored. Spectroscopic studies indicate that the compound has a good affinity for DNA and stains the nucleus of the cells.

1. Introduction

Transition-metal complexes having DNA interaction properties have attracted attention due to their potential applications, such as gene engineering, footprinting agents, sequence specific binding, structural probes and in drug development (Orvig & Abrams, 1999; Hambley, 2007; Liu *et al.*, 2004; Steinreiber & Ward, 2008; Jiang *et al.*, 2007; Pitié & Pratviel, 2010). These complexes offer a wide range of reactivities/properties due to their variable coordination number and geometries, available redox states, kinetic and thermodynamic properties and intrinsic properties of the metal ion and ligand itself. Cisplatin is one of the most widely used metal-based drugs in the treatment of various types of cancers (Boulikas & Vougiouka, 2003; Wong & Giandomenico, 1999; Jamieson & Lippard, 1999) and, although highly effective in the treatment of a variety of cancers, it possesses inherent limitations, such as serious side effects (Jung & Lippard, 2007), general toxicity and acquired drug resistance (Jamieson & Lippard, 1999). Because of these problems, considerable attempts have been made to develop alternative strategies based on different metals with improved pharmacological properties aimed at different targets (Bruijnincx & Sadler, 2008). Researchers have tried various transition-metal complexes, *viz.* Ru^{II}, Co^{II}, Zn^{II}, Ni^{II}, Cu^{II}, *etc.*, of which copper complexes have shown encouraging perspectives (Santini *et al.*, 2014; Tardito & Marchiò, 2009; Marzano *et al.*, 2009; Tisato *et al.*, 2010; Duncan & White, 2012). Copper, being a bio-essential metal ion, may be less toxic to normal cells than to cancer cells; its complexes with tunable coordination geometries in a redox-active

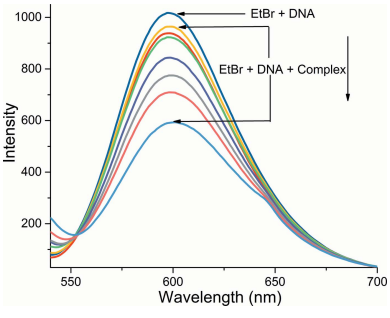

environment could find better application at the cellular level. The artificial nuclease activity of copper complexes has been studied frequently due to their high cleavage efficiency and alterable cleavage behaviour (Santini *et al.*, 2014; Sigman *et al.*, 1993; Maheswari *et al.*, 2008). Sigman and co-workers reported the first chemical nuclease based on a bis(1,10-phenanthroline)copper(I) complex that efficiently cleaves DNA in the presence of a reducing agent (Sigman *et al.*, 1993; Pope & Sigman, 1984; Sigman, 1990; Kuwabara & Sigman, 1987). In recent years, there has been a substantial increase in the design and study of DNA binding and cleavage properties of copper(II) complexes and the development of new copper-based metallodrugs (Santini *et al.*, 2014; Li *et al.*, 2009; Bhat *et al.*, 2011; Li *et al.*, 2011; Childs *et al.*, 2006; Rodríguez Solano *et al.*, 2011; Maheswari *et al.*, 2006).

The majority of copper complexes reported up to now have no intrinsic fluorescence to aid vizualization within the cell, so they need to be modified with a fluorescent tag to monitor their localization within the cell. In an effort to study the structure–activity relationships of copper complexes, we report herein the synthesis, structural characterization, DNA interaction properties, anticancer activity and cellular localization of the newly synthesized fluorophore-labelled copper complex $[Cu(ClO_4)(qip)(DMF)_2(H_2O)]ClO_4\cdot H_2O$, (I), where qip is 2-(quinolin-2-yl)-1,3-oxazolo[4,5-*f*][1,10]phenanthroline and DMF is dimethylformamide. Furthermore, we have structurally characterized a cyclic hybrid water–perchlorate cluster, *i.e.* $[(ClO_4)_2(H_2O)_2]^{2-}$, within the crystal structure of copper(II) complex (I).

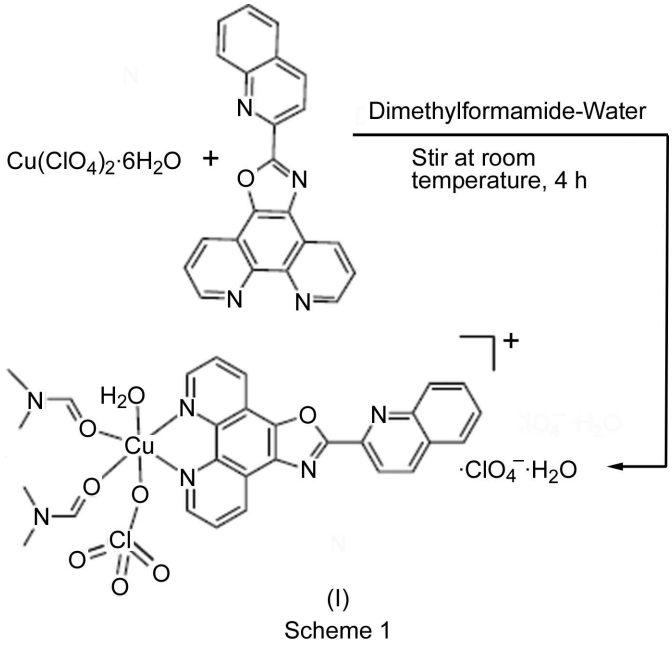

Scheme 1

2. Experimental

Dulbecco's Modified Eagle Medium (DMEM) was purchased from HiMedia Laboroteries Pvt. Ltd, Mumbai, India, and was used as received. 1,10-Phenanthroline-5,6-dione (phendione) was synthesized according to the literature procedure of Masaki *et al.* (1992). All chemicals and solvents were purchased commercially and were used as received. $Cu(ClO_4)_2\cdot 6H_2O$ and calf-thymus DNA (CT-DNA) were purchased from SRL, Kolkata (India), and used as received. Quinoline-2-carbaldehyde was purchased from Sigma–Aldrich, Bangalore, India. ^{1}H NMR spectra were recorded on a Jeol ECX-400 spectrometer at room temperature. The IR spectra of solid samples dispersed in KBr were recorded on a Nicolet USA model–Nicolet 6700 FT–IR spectrometer. Microanalysis (C, H and N) was carried out with a PerkinElmer 2400 series II analyzer. The absorption spectrum of the complex was measured on a Jasco V670 spectrophotometer and the emission spectra was measured on a Hitachi F-7000 at room temperature.

Table 1
Experimental details.

Crystal data	
Chemical formula	$[Cu(ClO_4)(C_{22}H_{12}N_4O)(C_3H_7NO)_2(H_2O)]ClO_4\cdot H_2O$
M_r	793.02
Crystal system, space group	Monoclinic, *C*2/*c*
Temperature (K)	173
a, *b*, *c* (Å)	48.675 (3), 8.3750 (5), 16.3155 (9)
β (°)	100.716 (2)
V (Å^3)	6535.1 (6)
Z	8
Radiation type	Cu *K*α
μ (mm^{-1})	3.12
Crystal size (mm)	0.28 × 0.22 × 0.17
Data collection	
Diffractometer	Bruker X8 Proteum
Absorption correction	Multi-scan (*SADABS*; Bruker, 2010)
T_{min}, T_{max}	0.482, 0.505
No. of measured, independent and observed [$I > 2\sigma(I)$] reflections	29422, 5417, 4790
R_{int}	0.071
(sin $\theta/\lambda)_{max}$ (Å^{-1})	0.586
Refinement	
$R[F^2 > 2\sigma(F^2)]$, $wR(F^2)$, *S*	0.047, 0.132, 1.02
No. of reflections	5417
No. of parameters	504
No. of restraints	157
H-atom treatment	H-atom parameters constrained
$\Delta\rho_{max}$, $\Delta\rho_{min}$ (e Å^{-3})	0.77, −0.48

Computer programs: *SAINT* (Bruker, 2010), *SMART* (Bruker, 2010), *SHELXT* (Sheldrick, 2015*a*), *SHELXL2014* (Sheldrick, 2015*b*) and *OLEX2* (Dolomanov *et al.*, 2009).

2.1. Synthesis and crystallization

2.1.1. Synthesis of 2-(quinolin-2-yl)-1,3-oxazolo[4,5-*f*]-[1,10]phenanthroline (qip). A mixture of quinoline-2-carbaldehyde (0.30 g, 1.91 mmol), 1,10-phenanthroline-5,6-dione (0.4 g, 1.91 mmol) and ammonium acetate (1.47 g, 19.1 mmol) in glacial acetic acid was refluxed for 4 h, then cooled to room temperature and diluted with cold water (30 ml). Addition of dilute aqueous ammonia gave a white product, which was collected by filtration and washed repeatedly with water. The crude product obtained was purified by recrystallization from methanol (yield: 495 mg, 75%). ^{1}H NMR (400 MHz, DMSO-

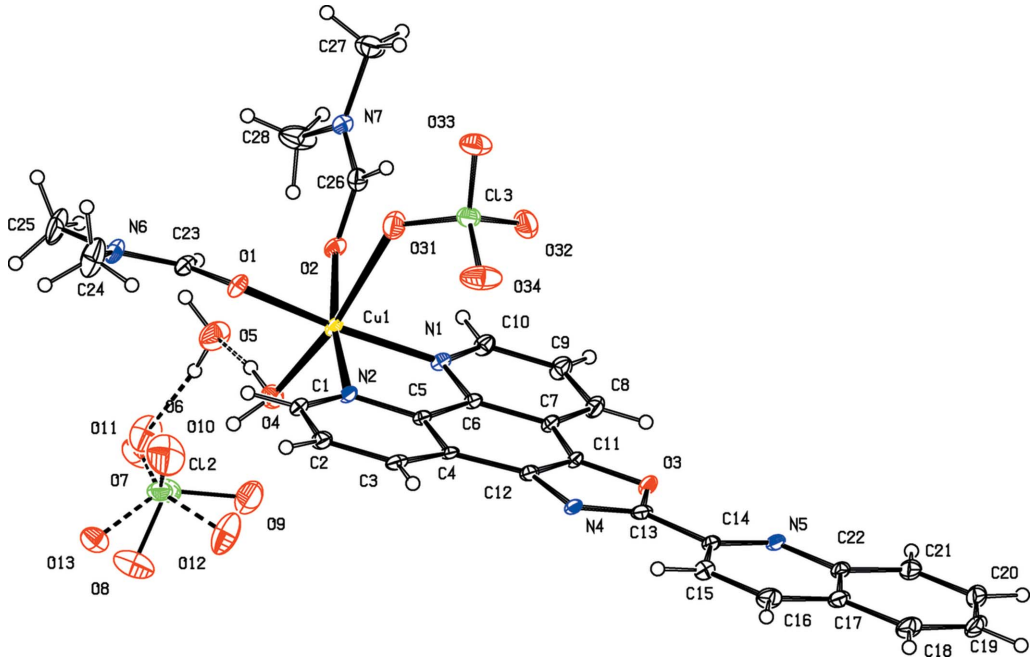

Figure 1
The molecular structure of complex (I). Displacement ellipsoids are draw at the 30% probability level. One of the perchlorate anions is disordered in a 2:1 ratio.

d_6): δ 9.20 (*m*, 2H), 8.97 (*dd*, 1H), 8.93 (*dd*, 1H), 8.69 (*d*, 1H), 8.58 (*d*, 1H), 8.27 (*d*, 1H), 8.13 (*d*, 1H), 7.95 (*m*, 3H), 7.68 (*t*, 1H). Analysis calculated (%) for $C_{22}H_{12}N_4O$: C 75.85, H 3.47, N 16.08%; found: C 75.91, H 3.53, N 15.97%.

2.1.2. Synthesis of $[Cu(ClO_4)(qip)(DMF)_2(H_2O)]ClO_4\cdot H_2O$, (I). To a solution of qip (0.2 g, 0.574 mmol) in DMF (5 ml) was added a solution of $Cu(ClO_4)_2\cdot 6H_2O$ (0.212 g, 0.574 mmol) in water (5 ml) with stirring. The solution immediately turned dark green and was stirred for 4 h at room temperature. The resulting solution was left to stand for slow evaporation at room temperature and single crystals of (I) were obtained after five weeks and collected by filtration (yield 0.320 g, 72%). Analysis calculated (%) for $C_{28}H_{30}Cl_2CuN_6O_{13}$: C 42.41, H 3.81, N 10.60%; found: C 42.32, H 3.85, N 10.47%. IR: 3440 (*bt*), 3055, 3008, 2928, 1667, 1614, 1544, 1520, 1447, 1143, 1109, 1080, 658, 626.

2.2. Refinement

Crystal data, data collection and structure refinement details are summarized in Table 1. H-atom positions were calculated geometrically and refined using a riding model. The free and bound water molecules were refined as rigid groups and with $U_{iso}(H) = 1.5U_{eq}(O)$. The perchlorate anion is disordered over two positions and was refined with fixed occupancies of $\frac{1}{3}$ and $\frac{2}{3}$ for Cl2/O6/O7/O8/O9 and Cl1/O10/O11/O13/O14, respectively, along with various bond and displacement-parameter restraints.

2.3. DNA binding studies

The concentration of CT-DNA was calculated from its known extinction coefficient at 260 nm (6600 M^{-1} cm^{-1}).

2.4. Ethidium bromide displacement assay

The apparent binding constant (K_{app}) of the complex was determined by competitive binding of (I) with ethidium bromide (EtBr) bound CT-DNA solution in phosphate buffer (pH 7.2). The changes in fluorescence intensities of EtBr (546 nm excitation) bound to DNA were monitored with an increasing concentration of (I). EtBr was non-emissive in phosphate buffer (pH 7.2) medium due to fluorescence quenching of the free EtBr by the solvent molecules. In the presence of DNA, EtBr showed enhanced emission intensity due to its intercalative binding to DNA. A competitive binding of the copper complex to CT-DNA resulted in the displacement of the bound EtBr, thus decreasing its emission intensity.

2.5. Emission titration

Emission titration experiments were carried out by the addition of an increasing concentration of DNA to the copper complex in the buffer. A typical concentration of metal complex used was 10 μM and [DNA]/[Cu] ratios were in the range 0–20. Before the measurement of the emission spectra, the DNA–complex solution was allowed to react for 15 min.

2.6. Cytotoxicity: cell-viability assay

The cell viability after appropriate treatment was determined with a 3-(4,5-dimethylthiazol-2-yl)-2,5-diphenyltetrazolium bromide (MTT; Sigma Chemical Co.) assay (Chen *et al.*, 2004). Briefly, cells were plated (4000 cells/well per 0.2 ml DMEM medium) in 96-well microtiter plates and incubated overnight. Complex (I) was then added at indicated concentrations to quadruplicate wells. After a reaction time of 48 h, MTT was added to each well at a final volume of 0.5 mg ml^{-1}

and the microplates were incubated at 310 K for 3 h. After that, the supernatant was removed, the formazan salt resulting from the reduction of MTT was solubilized in dimethyl sulfoxide (DMSO, Sigma Chemical Co.) and the absorbance was read at 570 nm using an automatic plate reader (Thermo Corporation). The cell viability was extrapolated from optical density (OD) 570 nm values and expressed as percent survival.

2.7. Fluorescence microscopy studies

Hela Cells were grown on sterile glass cover slips in a 35 mm tissue culture dish and incubated at 310 K under a 5% CO_2 atmosphere for 48 h. The culture medium was replaced with a medium containing a 10 μ*M* concentration of complex (I). After incubation for 1 h, the cells were washed gently with PBS (3 × 2 ml; PBS is phosphate buffered saline). After washing with PBS, the cover slips were mounted onto slides for the measurements. The images were taken in a Carl Zeiss Axio Scope A1 fluorescence microscope.

For DAPI costaining (DAPI is 4′,6-diamidino-2-phenylindole), the cells were washed and incubated with a medium containing 10 μ*M* complex (I) for 1 h at 310 K under 5% CO_2. The cells were washed with PBS and cultured with a medium containing DAPI (1 μg ml^{-1}) for another 5 min. Cell-imaging experiments were then performed after the cells were washed with PBS three times.

3. Results and discussion

3.1. Synthesis and characterization

2-(Quinolin-2-yl)-1,3-oxazolo[4,5-*f*][1,10]phenanthroline (qip) was synthesized by condensation of 1,10-phenanthroline-5,6-dione with quinoline-2-carbaldehyde in the presence of ammonium acetate in glacial acetic acid. The crude product obtained was purified by column chromatography and characterized by IR, ^{1}H NMR and mass and elemental analyses. The corresponding copper complex was synthesized by reaction of copper perchlorate with qip in DMF in a 1:1 molar ratio (see Scheme 1). Complex (I) was characterized by IR spectroscopy, elemental analysis, UV–Visible spectroscopy and single-crystal X-ray structure determination.

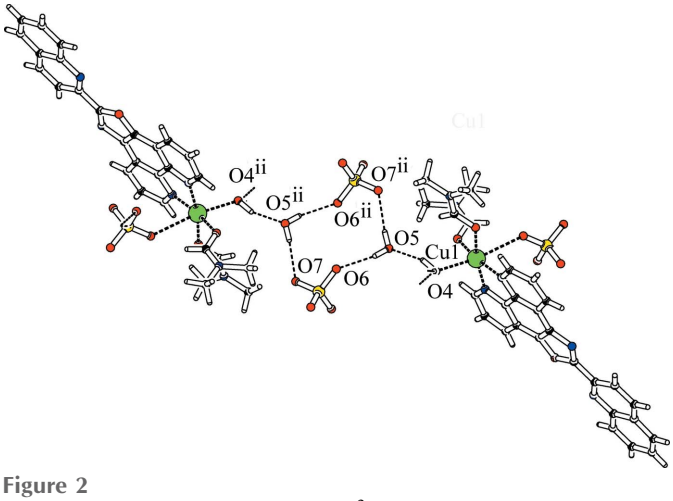

Figure 2
A view of the cyclic $[(H_2O)_2(ClO_4)_2]^{2-}$ cluster in (I). Only the major disorder form of the perchlorate anion is shown. [Symmetry code: (ii) $-x+\frac{3}{2}, -y+\frac{1}{2}, -z+1$.]

3.2. Crystal structure

Single crystals of complex (I) suitable for X-ray diffraction were grown by slow evaporation of the complex in a DMF and water mixture at room temperature. Complex (I) crystallized in the monoclinic crystal system with the *C*2/*c* space group and the molecular structure is shown in Fig. 1. The Cu^{II} atom is six-coordinated, with an N_2O_4 donor set, forming a distorted octahedral geometry. The mean Cu—N distance is 2.00 (2) Å and the N—Cu—N bite angle is 82.09 (9)°, which is similar to the values reported for similar copper complexes (Bhat *et al.*, 2011; Onawumi *et al.*, 2008).

3.3. Cyclic hybrid water–perchlorate cluster in (I)

Recently, the recognition of hydrated forms of anions has attracted a great deal of attention due to their role in many chemical, environmental and biological processes (Chen *et al.*, 2013; Mascal *et al.*, 2006). Inorganic anions are familiar in nature and take part in natural processes occurring in water (Ohmine & Saito, 1999; Ludwig, 2001). Thus, the structural characterization of inorganic anion–water clusters is of vital importance for understanding the hydration phenomena of

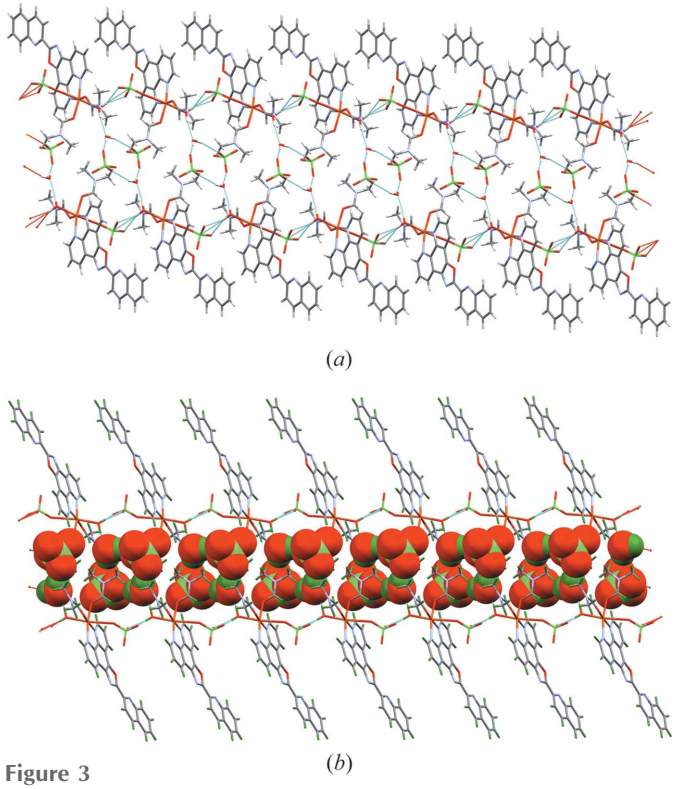

Figure 3
Crystal packing diagrams of complex (I), showing (*a*) the water–perchlorate cluster channels and (*b*) a spacefilling model showing the water–perchlorate-filled channel. The views are approximately along the *c* axis.

Table 2
Hydrogen-bond geometry (Å, °).

D—H···A	D—H	H···A	D···A	D—H···A
O4—H4A···O5	0.91	1.94	2.808 (3)	160
O4—H4B···O32^{i}	0.91	1.96	2.782 (3)	151
O5—H5A···O11^{ii}	0.85	2.02	2.862 (18)	170
O5—H5B···O10	0.85	1.95	2.790 (13)	171
O5—H5A···O7^{ii}	0.85	2.11	2.954 (7)	174
O5—H5B···O6	0.85	2.07	2.905 (7)	165

Symmetry codes: (i) $x, y-1, z$; (ii) $-x+\frac{3}{2}, -y+\frac{1}{2}, -z+1$.

inorganic anions in nature and biological systems (Sodaye *et al.*, 2006; Kumar *et al.*, 2011). Inorganic anion–water clusters remain relatively unexplored compared to the large number of reports on water clusters (Barbour *et al.*, 1998; Moorthy *et al.*, 2002; Dai *et al.*, 2008; Jin *et al.*, 2010). In the case of inorganic anion–water clusters, most of the studies reported up to now have focused on water–chloride clusters in a variety of crystal systems, examples being $\{[(H_2O)_{20}Cl_4]^{4-}\}_n$ (Fernandes *et al.*, 2008), $[(H_2O)_6Cl_2]^{2-}$ (Butchard *et al.*, 2006), $[(H_2O)_{10}Cl_2]^{2-}$ (Mascal *et al.*, 2006), $\{[(H_2O)_4Cl_2]^{2-}\}_n$ (Saha & Bernal, 2005), $\{[(H_2O)_6Cl_2]^{2-}\}_n$ (Saha & Bernal, 2005), $\{[(H_2O)_7(HCl)_2]^{2-}\}_n$ (Prabhakar *et al.*, 2006), $\{[(H_2O)_{11}Cl_7]^{7-}\}_n$ (Lakshminarayanan *et al.*, 2006), $\{[(H_2O)_{14}Cl_5]^{5-}\}_n$ (Deshpande *et al.*, 2006, $\{[(H_2O)_{18}Cl_8]^{8-}\}_n$ (Bhat & Revankar, 2016), $\{[(H_2O)_{10}Cl_2]^{2-}\}_n$ (Bhat *et al.*, 2015) and $\{[(H_2O)_{14}Cl_4]^{4-}\}_n$ (Reger *et al.*, 2006). To the best of our knowledge, there are only a few reports on discrete perchlorate–water clusters, which include $[H_2O)_2(ClO_4)_2]^{2-}$ (Hedayetullah Mir & Vittal, 2008; Li *et al.*, 2012).

Interestingly, the crystal structure packing of complex (I) contains extensive hydrogen-bonding interactions between the lattice water molecules and the perchlorate anions (Table 2), leading to the formation of an anionic hybrid cyclic water–perchlorate cluster, *i.e.* the $[(H_2O)_2(ClO_4)_2]^{2-}$ unit shown in Fig. 2. Each anionic cyclic cluster is made up of two water molecules and two perchlorate anions, and is interconnected by hydrogen bonding with the cationic units. Anion–water clusters are stabilized by hydrogen bonding involving the coordinated water and perchlorate ligand of the cationic complex. Further intermolecular hydrogen bonding in the crystal packing leads to the formation of a nonpolar one-dimensional water–perchlorate anionic channel, as shown in Fig. 3. In the crystal packing of (I), the one-dimensional anionic hybrid water–perchlorate $[(H_2O)_2(ClO_4)_2]^{2-}$ clusters occupy the free space between the hydrophobic arrays of the metal–organic part, with an interlayer separation of 11.22 Å. A spacefilling model of the packing (Fig. 3*b*) shows the water–chloride clusters along the *b* axis. Selected hydrogen-bonding parameters are given in Table 2.

3.4. Photophysical properties

The absorption and emission spectra of (I) are given in Fig. 4. The electronic spectrum of the complex recorded in DMF is dominated by high-energy bands in the region 220–350 nm attributed to $\pi\rightarrow\pi^*$ transitions of the aromatic quinoline-containing nitrogen-donor ligand (Li *et al.*, 2014;

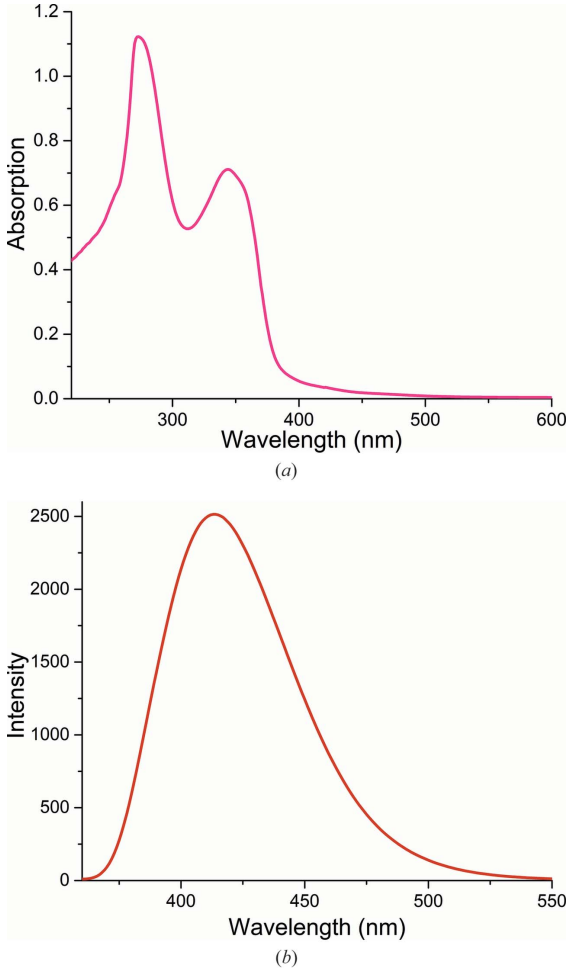

Figure 4
The (*a*) absorption and (*b*) emission spectra of (I) in dimethylformamide. The excitation wavelength is 350 nm.

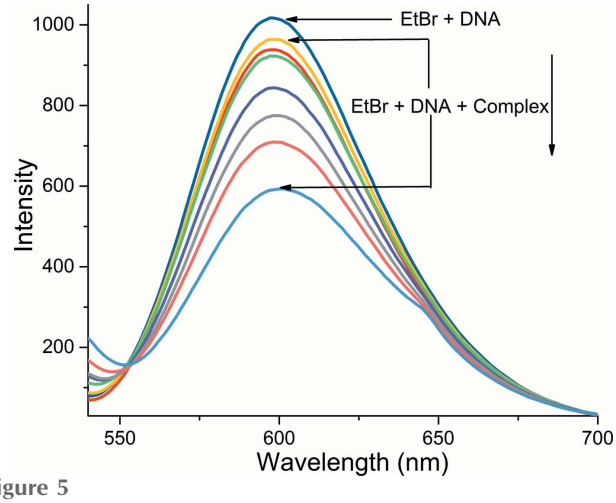

Figure 5
The effect of the addition of an increasing concentration of (I) on the emission intensity of the EtBr-bound CT-DNA phosphate buffer (pH 7.2); [EtBr] = 20 μ*M* and [DNA] = 20 μ*M*. The decrease in emission intensity from highest to lowest corresponds to successive addition of 0, 5, 10, 20, 30, 40, 60 and 100 μ*M* of (I).

Rajendiran *et al.*, 2007). Compound (I) is highly fluorescent (Fig. 4*b*), with the emission centred around 430 nm. Interestingly, no quenching of the fluorescence is observed in water.

3.5. Ethidium bromide (EtBr) displacement assay

To study the DNA interaction properties of (I), a competitive binding assay was performed. For competitive binding studies, changes in the emission intensity of EtBr bound to DNA were monitored as a function of an increasing concentration of (I). Emission of EtBr in the buffer solution is completely quenched by solvent molecules (Dhar *et al.*, 2005), but it emits intensively in the presence of DNA due to the strong intercalative mode of binding with DNA (Meyer-Almes & Porschke, 1993). The enhanced fluorescence of EtBr bound to DNA can be quenched by the addition of another molecule (Baguley & Le Bret, 1984); this reduction in the emission intensity is *via* the replacement of a molecular fluorophore (Pasternack *et al.*, 1991). An appreciable decrease in fluorescence intensity was observed upon addition of (I) to the EtBr–DNA solution (Fig. 5), which was due to intercalation of (I) with DNA by replacement of EtBr molecules bound to DNA. The apparent binding constant (K_{app}) has been calculated from equation (1) (Lee *et al.*, 1993),

$$K_{EtBr}[EtBr] = K_{app}[Complex], \quad (1)$$

where K_{EtBr} is $1 \times 10^7\ M^{-1}$ and the concentration of EtBr is 20 µ*M*; [Complex] represents the concentration of the complex causing a 50% reduction in the emission intensity of EtBr. The K_{app} value for (I) is $2 \times 10^6\ M^{-1}$. The higher values of K_{app} indicate that this complex binds strongly to DNA.

3.6. Emission titration

Changes in the emission spectra of complexes in the presence of DNA are a diagnostic means to determine DNA binding (Deshpande *et al.*, 2009; Bhat *et al.*, 2010; Pellegrini & Aldrich-Wright, 2003). The changes in the steady-state emission spectra of (I) with successive addition of CT-DNA (phosphate buffer pH 7.2) are shown in Fig. 6.

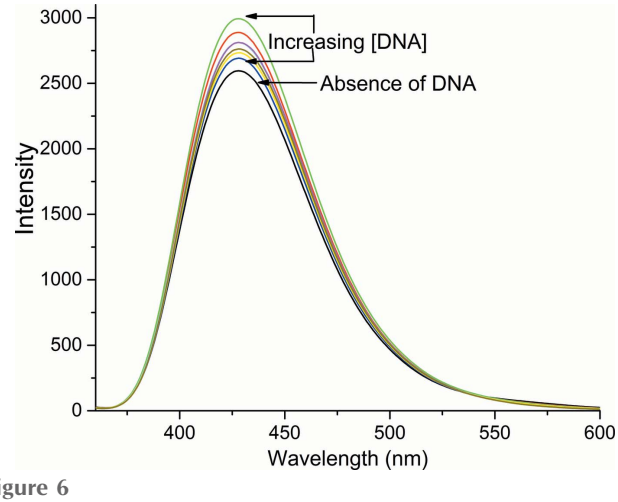

Figure 6
Emission spectra of (I) (10 µ*M*) with increasing [CT-DNA]/[Cu] ratio (0–20) in phosphate buffer (pH 7.2) at 298 K.

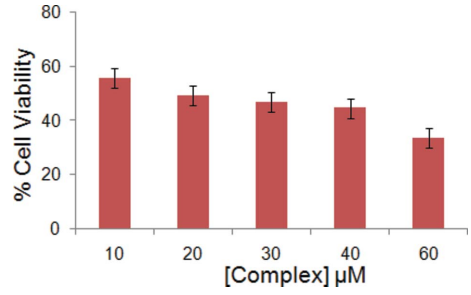

Figure 7
Cytotoxicity evaluation of (I) against the HeLa cell line. The cell viability was measured after 48 h by MTT assay. Each data point represents the mean of three separate experiments. The units for [Complex] are µ*M*.

3.7. Cytotoxicity studies

The *in vitro* cytotoxicity of complex (I) against the cancer cell line HeLa (cerevical) has been tested by MTT [3-(4,5-dimethylthiazol-2-yl)-2,5-diphenyltetrazolium bromide] assay. Complex (I) exhibits significant cytotoxicity in a concentration-dependent manner (Fig. 7). The percent cell viability of the HeLa cells in the presence of (I) was measured in the concentration range 10–60 µ*M*, wherein the compound tested was found to be active at lower concentrations. The IC_{50} value is 20±0.08 µ*M* for (I), which is similar to the value reported for $[Cu_2(1,4\text{-tpbd})(DMSO)_2(ClO_4)_2](OH)_2{\cdot}6H_2O$ and $[Cu_2(1,4\text{-tpbd})(OAC)_2(ClO_4)_2]{\cdot}5H_2O$ [1,4-tpbd is *N*,*N*,*N*′,*N*′-tetrakis(pyridin-2-ylmethyl)benzene-1,4-diamine], with IC_{50} values of 13.67 and 16.58 µ*M*, respectively, against the HeLa cell line (Li *et al.*, 2011).

3.8. Cellular uptake and cellular localization studies

The cellular uptake of complex (I) was monitored using fluorescence microscopy because of its intrinsic fluorescence. One of the advantages of this complex for fluorescence microscopy is that there is no overlap between the absorption and emission spectra, since the overlap of spectra results in interference of the excitation light in the collection of the emission image, which decreases the image contrast. As shown in Fig. 8 the complex stains the nucleus of the cells.

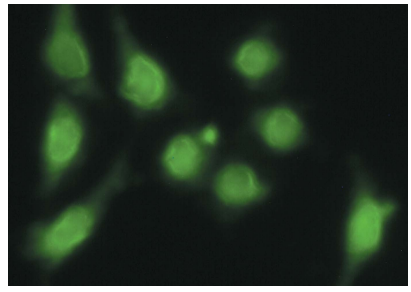

Figure 8
Fluorescence microscopy image of HeLa cells incubated (for 1 h) with 10 µ*M* of (I).

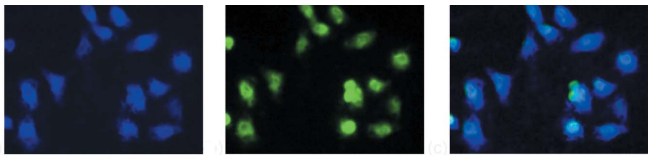

(*a*) (*b*) (*c*)

Figure 9
Fluorescence microscopy images of HeLa cells incubated (for 1 h) with 10 μ*M* of (I) and the DNA-specific stain DAPI, shown (*a*) with (I), (*b*) with DAPI and (*c*) as an overlay image.

Furthermore, to confirm the nuclear localization of the complex, a costaining experiment with commercially available nuclear staining DAPI was carried out. As shown in Fig. 9, complete overlap of the DAPI and complex signals within the cells confirms the nuclear localization of the complex within the cells.

Acknowledgements

The authors thank SIF, NMR Research Centre, IISC Bangalore, CDRI–Lucknow, USIC Karnatak University, Dharwad, and Institute of Excellence, University of Mysore, India, for providing NMR, ESI–MS data and single-crystal X-ray data.

Funding information

Funding for this research was provided by: Science and Engineering Research Board, Department of Science and Technology, New Delhi, India (Start-Up-Grant (Young Scientist) project No. YSS/2014/000546 to SB).

References

Baguley, B. C. & Le Bret, M. (1984). *Biochemistry*, **23**, 937–943.
Barbour, L. J., Orr, G. W. & Atwood, J. L. (1998). *Nature*, **393**, 671–673.
Bhat, S. S., Kumbhar, A. A., Heptullah, H., Khan, A. A., Gobre, V. V., Gejji, S. P. & Puranik, V. G. (2011). *Inorg. Chem.* **50**, 545–558.
Bhat, S. S., Kumbhar, A. S., Lönnecke, P. & Hey-Hawkins, E. (2010). *Inorg. Chem.* **49**, 4843–4853.
Bhat, S. S. & Revankar, V. K. (2016). *J. Chem. Crystallogr.* **46**, 9–14.
Bhat, S. S., Revankar, V. K., Khan, A., Butcher, R. J. & Thatipamula, K. (2015). *New J. Chem.* **39**, 3646–3657.
Boulikas, T. & Vougiouka, M. (2003). *Oncol. Rep.* **10**, 1663–1682.
Bruijnincx, P. C. & Sadler, P. J. (2008). *Curr. Opin. Chem. Biol.* **12**, 197–206.
Bruker (2010). *SMART*, *SAINT* and *SADABS*. Bruker AXS Inc., Madison, Wisconsin, USA.
Butchard, J. R., Curnow, O. J., Garrett, D. J. & Maclagan, R. G. A. R. (2006). *Angew. Chem. Int. Ed.* **45**, 7550–7553.
Chen, J. S., Konopleva, M., Andreeff, M., Multani, A. S., Pathak, S. & Mehta, K. (2004). *J. Cell. Physiol.* **200**, 223–234.
Chen, W., Long, L., Huang, R. & Zheng, L. (2013). *Cryst. Growth Des.* **13**, 2507–2513.
Childs, L. J., Malina, J., Rolfsnes, B. E., Pascu, M., Prieto, M. J., Broome, M. J., Rodger, P. M., Sletten, E., Moreno, V., Rodger, A. & Hannon, M. J. (2006). *Chem. Eur. J.* **12**, 4919–4927.
Dai, F., He, H. & Sun, D. (2008). *J. Am. Chem. Soc.* **130**, 14064–14065.
Deshpande, M. S., Kumbhar, A. A., Kumbhar, A. S., Kumbhakar, M., Pal, H., Sonawane, U. B. & Joshi, R. R. (2009). *Bioconjugate Chem.* **20**, 447–459.
Deshpande, M. S., Kumbhar, A. S., Puranik, V. G. & Selvaraj, K. (2006). *Cryst. Growth Des.* **6**, 743–748.
Dhar, S., Nethaji, M. & Chakravarty, A. R. (2005). *J. Inorg. Biochem.* **99**, 805–812.
Dolomanov, O. V., Bourhis, L. J., Gildea, R. J., Howard, J. A. K. & Puschmann, H. (2009). *J. Appl. Cryst.* **42**, 339–341.
Duncan, C. & White, A. R. (2012). *Metallomics*, **4**, 127–138.
Fernandes, R. R., Kirillov, A. M., da Silva, M. F. C. G., Ma, Z., da Silva, J. A. L., da Silva, J. J. R. F. & Pombeiro, A. J. L. (2008). *Cryst. Growth Des.* **8**, 782–785.
Hambley, T. W. (2007). *Dalton Trans.* pp. 4929–4937.
Hedayetullah Mir, M. & Vittal, J. J. (2008). *Cryst. Growth Des.* **8**, 1478–1480.
Jamieson, E. R. & Lippard, S. J. (1999). *Chem. Rev.* **99**, 2467–2498.
Jiang, Q., Xiao, N., Shi, P., Zhu, Y. & Guo, Z. (2007). *Coord. Chem. Rev.* **251**, 1951–1972.
Jin, C.-M., Zhu, Z., Chen, Z.-F., Hu, Y.-J. & Meng, X.-G. (2010). *Cryst. Growth Des.* **10**, 2054–2056.
Jung, Y. & Lippard, S. J. (2007). *Chem. Rev.* **107**, 1387–1407.
Kumar, R., Pandey, A. K., Sharma, M. K., Panicker, L. V., Sodaye, S., Suresh, G., Ramagiri, S. V., Bellare, J. R. & Goswami, A. (2011). *J. Phys. Chem. B*, **115**, 5856–5867.
Kuwabara, M. D. & Sigman, D. S. (1987). *Biochemistry*, **26**, 7234–7238.
Lakshminarayanan, P. S., Suresh, E. & Ghosh, P. (2006). *Angew. Chem. Int. Ed.* **45**, 3807–3811.
Lee, M., Rhodes, A. L., Wyatt, M. D., Forrow, S. & Hartley, J. A. (1993). *Biochemistry*, **32**, 4237–4245.
Li, M.-J., Lan, T.-Y., Cao, X.-H., Yang, H.-H., Shi, Y., Yi, C. & Chen, G.-N. (2014). *Dalton Trans.* **43**, 2789–2798.
Li, D.-D., Tian, J.-L., Gu, W., Liu, X., Zeng, H.-H. & Yan, S.-P. (2011). *J. Inorg. Biochem.* **105**, 894–901.
Li, D., Tian, J., Kou, Y., Huang, F., Chen, G., Gu, W., Liu, X., Liao, D., Cheng, P. & Yan, S. (2009). *Dalton Trans.* pp. 3574–3583.
Li, Z.-Y., Yang, J.-S., Liu, R.-B., Zhang, J.-J., Liu, S.-Q., Ni, J. & Duan, C.-Y. (2012). *Dalton Trans.* **41**, 13264–13266.
Liu, C., Wang, M., Zhang, T. & Sun, H. (2004). *Coord. Chem. Rev.* **248**, 147–168.
Ludwig, R. (2001). *Angew. Chem. Int. Ed.* **40**, 1808–1827.
Maheswari, P. U., Roy, S., den Dulk, H., Barends, S., van Wezel, G., Kozlevčar, B., Gamez, P. & Reedijk, J. (2006). *J. Am. Chem. Soc.* **128**, 710–711.
Maheswari, P. U., van der Ster, M., Smulders, S., Barends, S., van Wezel, G. P., Massera, C., Roy, S., den Dulk, H., Gamez, P. & Reedijk, J. (2008). *Inorg. Chem.* **47**, 3719–3727.
Marzano, C., Pellei, M., Tisato, F. & Santini, C. (2009). *Anticancer Agents Med. Chem.* **9**, 185–211.
Masaki, Y., Yoshihito, T., Yasuyuki, Y., Shigeyasu, K. & Ichiro, S. (1992). *Bull. Chem. Soc. Jpn*, **65**, 1006–1011.
Mascal, M., Infantes, L. & Chisholm, J. (2006). *Angew. Chem. Int. Ed.* **45**, 32–36.
Meyer-Almes, F. J. & Porschke, D. (1993). *Biochemistry*, **32**, 4246–4253.
Moorthy, J. N., Natarajan, R. & Venugopalan, P. (2002). *Angew. Chem. Int. Ed.* **41**, 3417–3420.
Ohmine, I. & Saito, S. (1999). *Acc. Chem. Res.* **32**, 741–749.
Onawumi, O. O. E., Faboya, O. O. P., Odunola, O. A., Prasad, T. K. & Rajasekharan, M. V. (2008). *Polyhedron*, **27**, 113–117.
Orvig, C. & Abrams, M. J. (1999). *Chem. Rev.* **99**, 2201–2204.
Pasternack, R. F., Caccam, M., Keogh, B., Stephenson, T. A., Williams, A. P. & Gibbs, E. J. (1991). *J. Am. Chem. Soc.* **113**, 6835–6840.
Pellegrini, P. P. & Aldrich-Wright, J. R. (2003). *Dalton Trans.* pp. 176–183.
Pitié, M. & Pratviel, G. (2010). *Chem. Rev.* **110**, 1018–1059.
Pope, L. E. & Sigman, D. S. (1984). *Proc. Natl Acad. Sci. USA*, **81**, 3–7.
Prabhakar, M., Zacharias, P. S. & Das, S. K. (2006). *Inorg. Chem. Commun.* **9**, 899–902.
Rajendiran, V., Karthik, R., Palaniandavar, M., Stoeckli-Evans, H., Periasamy, V. S., Akbarsha, M. A., Srinag, B. S. & Krishnamurthy, H. (2007). *Inorg. Chem.* **46**, 8208–8221.

Reger, D. L., Semeniuc, R. F., Pettinari, C., Luna-Giles, F. & Smith, M. D. (2006). *Cryst. Growth Des.* **6**, 1068–1070.
Rodríguez Solano, L. A., Aguiñiga, I., López Ortiz, M., Tiburcio, R., Luviano, A., Regla, I., Santiago-Osorio, E., Ugalde-Saldívar, V. M., Toscano, R. A. & Castillo, I. (2011). *Eur. J. Inorg. Chem.* pp. 3454–3460.
Saha, M. K. & Bernal, I. (2005). *Inorg. Chem. Commun.* **8**, 871–873.
Santini, C., Pellei, M., Gandin, V., Porchia, M., Tisato, F. & Marzano, C. (2014). *Chem. Rev.* **114**, 815–862.
Sheldrick, G. M. (2015). *Acta Cryst.* C**71**, 3–8.
Sigman, D. S. (1990). *Biochemistry*, **29**, 9097–9105.
Sigman, D. S., Mazumder, A. & Perrin, D. M. (1993). *Chem. Rev.* **93**, 2295–2316.
Sodaye, S., Suresh, G., Pandey, A. K. & Goswami, A. (2006). *Radiochim. Acta*, **94**, 347–350.
Steinreiber, J. & Ward, T. R. (2008). *Coord. Chem. Rev.* **252**, 751–766.
Tardito, S. & Marchiò, L. (2009). *Curr. Med. Chem.* **16**, 1325–1348.
Tisato, F., Marzano, C., Porchia, M., Pellei, M. & Santini, C. (2010). *Med. Res. Rev.* **30**, 708–749.
Wong, E. & Giandomenico, C. M. (1999). *Chem. Rev.* **99**, 2451–2466.

supporting information

Acta Cryst. (2017). C**73**, 710-717 [https://doi.org/10.1107/S2053229617011639]

A fluorophore-labelled copper complex: crystal structure, hybrid cyclic water–perchlorate cluster and biological properties

Satish S. Bhat, Vidyanand K. Revankar, Naveen Shivalingegowda and N. K. Lokanath

Computing details

Data collection: *SAINT* (Bruker, 2010); cell refinement: *SMART* (Bruker, 2010); data reduction: *SAINT* (Bruker, 2010); program(s) used to solve structure: SHELXT (Sheldrick, 2015a); program(s) used to refine structure: *SHELXL2014* (Sheldrick, 2015b); molecular graphics: *OLEX2* (Dolomanov *et al.*, 2009); software used to prepare material for publication: *OLEX2* (Dolomanov *et al.*, 2009).

Aquabis(dimethylformamide-κO)(perchlorato-κO)[2-(quinolin-2-yl)-1,3-oxazolo[4,5-*f*][1,10]phenanthroline]copper(II) perchlorate monohydrate

Crystal data

$[Cu(ClO_4)(C_{22}H_{12}N_4O)(C_3H_7NO)_2(H_2O)]ClO_4·H_2O$
M_r = 793.02
Monoclinic, *C*2/*c*
a = 48.675 (3) Å
b = 8.3750 (5) Å
c = 16.3155 (9) Å
β = 100.716 (2)°
V = 6535.1 (6) Å^3
Z = 8
F(000) = 3256
D_x = 1.612 Mg m^{-3}
Cu *K*α radiation, λ = 1.54178 Å
Cell parameters from 4790 reflections
θ = 1.9–64.5°
μ = 3.12 mm^{-1}
T = 173 K
Rectangle, green
0.28 × 0.22 × 0.17 mm

Data collection

Bruker X8 Proteum diffractometer
φ and ω scans
Absorption correction: multi-scan (SADABS; Bruker, 2010)
T_{min} = 0.482, T_{max} = 0.505
29422 measured reflections
5417 independent reflections
4790 reflections with $I > 2\sigma(I)$
R_{int} = 0.071
θ_{max} = 64.5°, θ_{min} = 5.4°
h = −56→54
k = −9→9
l = −15→19

Refinement

Refinement on F^2
Least-squares matrix: full
$R[F^2 > 2\sigma(F^2)]$ = 0.047
$wR(F^2)$ = 0.132
S = 1.02
5417 reflections
504 parameters
157 restraints
Hydrogen site location: mixed
H-atom parameters constrained
$w = 1/[\sigma^2(F_o^2) + (0.0731P)^2 + 16.1488P]$ where $P = (F_o^2 + 2F_c^2)/3$
$(\Delta/\sigma)_{max}$ = 0.002
$\Delta\rho_{max}$ = 0.77 e Å^{-3}
$\Delta\rho_{min}$ = −0.48 e Å^{-3}

Special details

Geometry. All esds (except the esd in the dihedral angle between two l.s. planes) are estimated using the full covariance matrix. The cell esds are taken into account individually in the estimation of esds in distances, angles and torsion angles; correlations between esds in cell parameters are only used when they are defined by crystal symmetry. An approximate (isotropic) treatment of cell esds is used for estimating esds involving l.s. planes.

Fractional atomic coordinates and isotropic or equivalent isotropic displacement parameters (Å²)

	x	*y*	*z*	U_{iso}*/U_{eq}	Occ. (<1)
Cu1	0.63808 (2)	0.76800 (5)	0.33515 (3)	0.01822 (15)	
O2	0.67770 (4)	0.8210 (3)	0.37130 (13)	0.0231 (5)	
O1	0.64467 (4)	0.6953 (3)	0.22641 (13)	0.0232 (5)	
O3	0.54145 (4)	1.1271 (2)	0.48962 (12)	0.0212 (4)	
O4	0.65005 (5)	0.5336 (3)	0.39334 (14)	0.0283 (5)	
H4A	0.668680	0.514138	0.399543	0.042*	
H4B	0.641311	0.452483	0.362216	0.042*	
N2	0.59662 (5)	0.7598 (3)	0.29512 (15)	0.0172 (5)	
N1	0.62665 (5)	0.8758 (3)	0.43273 (14)	0.0187 (5)	
N4	0.51555 (5)	1.0462 (3)	0.36830 (15)	0.0176 (5)	
N7	0.71619 (5)	0.9632 (3)	0.36123 (16)	0.0231 (6)	
N5	0.49830 (5)	1.2951 (3)	0.53244 (15)	0.0189 (5)	
O5	0.70583 (5)	0.4386 (3)	0.44686 (19)	0.0468 (7)	
H5A	0.718900	0.438323	0.418626	0.070*	
H5B	0.706890	0.347375	0.470057	0.070*	
N6	0.66992 (5)	0.5341 (3)	0.15751 (17)	0.0284 (6)	
C5	0.58248 (5)	0.8501 (3)	0.34240 (17)	0.0164 (6)	
C6	0.59897 (6)	0.9109 (3)	0.41920 (18)	0.0171 (6)	
C4	0.55404 (5)	0.8880 (3)	0.31771 (17)	0.0171 (6)	
C1	0.58274 (6)	0.7023 (3)	0.22309 (18)	0.0195 (6)	
H1	0.592133	0.636716	0.191453	0.023*	
C26	0.68925 (6)	0.9459 (4)	0.35209 (19)	0.0236 (7)	
H26	0.677914	1.030785	0.330107	0.028*	
C3	0.54021 (6)	0.8312 (3)	0.23980 (18)	0.0196 (6)	
H3	0.521589	0.857181	0.219960	0.024*	
C11	0.55818 (6)	1.0365 (3)	0.44858 (18)	0.0183 (6)	
C23	0.66611 (6)	0.6122 (4)	0.22322 (19)	0.0234 (7)	
H23	0.679992	0.606736	0.270749	0.028*	
C22	0.47685 (6)	1.3819 (3)	0.55422 (19)	0.0209 (6)	
C7	0.58712 (6)	1.0027 (3)	0.47580 (18)	0.0186 (6)	
C13	0.51640 (6)	1.1273 (3)	0.43692 (19)	0.0208 (6)	
C12	0.54243 (6)	0.9866 (3)	0.37484 (18)	0.0184 (6)	
C2	0.55461 (6)	0.7368 (4)	0.19342 (19)	0.0212 (6)	
H2	0.545639	0.695999	0.142404	0.025*	
C8	0.60458 (6)	1.0527 (4)	0.54982 (19)	0.0246 (7)	
H8	0.597389	1.111196	0.589469	0.030*	
C15	0.46711 (6)	1.2196 (4)	0.4050 (2)	0.0227 (6)	
H15	0.464676	1.164073	0.354847	0.027*	
C10	0.64288 (6)	0.9274 (4)	0.50227 (19)	0.0228 (6)	

H10	0.661922	0.905087	0.511060	0.027*	
C17	0.44993 (6)	1.3887 (4)	0.5025 (2)	0.0242 (7)	
C14	0.49310 (6)	1.2182 (3)	0.46072 (18)	0.0181 (6)	
C9	0.63232 (6)	1.0138 (4)	0.5625 (2)	0.0263 (7)	
H9	0.644151	1.045097	0.611341	0.032*	
C16	0.44565 (6)	1.3050 (4)	0.4270 (2)	0.0269 (7)	
H16	0.428264	1.307446	0.391828	0.032*	
C21	0.48177 (7)	1.4658 (4)	0.6303 (2)	0.0278 (7)	
H21	0.499320	1.461098	0.664476	0.033*	
C18	0.42873 (7)	1.4798 (4)	0.5304 (2)	0.0339 (8)	
H18	0.410916	1.484971	0.497807	0.041*	
C20	0.46102 (8)	1.5540 (4)	0.6545 (2)	0.0364 (9)	
H20	0.464707	1.610582	0.704394	0.044*	
C19	0.43436 (8)	1.5600 (4)	0.6050 (3)	0.0396 (9)	
H19	0.420330	1.618773	0.622661	0.048*	
C27	0.72853 (8)	1.1103 (4)	0.3384 (2)	0.0389 (8)	
H27A	0.713995	1.185541	0.317883	0.058*	
H27B	0.739200	1.088833	0.295681	0.058*	
H27C	0.740586	1.153987	0.386435	0.058*	
C24	0.64950 (9)	0.5388 (6)	0.0826 (3)	0.0556 (12)	
H24A	0.632332	0.581308	0.094368	0.083*	
H24B	0.646343	0.432703	0.060585	0.083*	
H24C	0.656075	0.605475	0.042465	0.083*	
C28	0.73515 (7)	0.8364 (5)	0.3937 (3)	0.0517 (11)	
H28A	0.725217	0.755903	0.418378	0.078*	
H28B	0.749954	0.878560	0.435268	0.078*	
H28C	0.742904	0.790148	0.349225	0.078*	
C25	0.69518 (9)	0.4426 (5)	0.1565 (3)	0.0512 (11)	
H25A	0.707412	0.451478	0.209748	0.077*	
H25B	0.704433	0.483256	0.113808	0.077*	
H25C	0.690400	0.332488	0.145403	0.077*	
Cl3	0.61575 (2)	1.19401 (9)	0.26661 (5)	0.0271 (2)	
O32	0.62515 (6)	1.2378 (3)	0.35322 (16)	0.0436 (6)	
O31	0.62935 (5)	1.0488 (3)	0.25143 (15)	0.0358 (6)	
O33	0.62201 (5)	1.3185 (3)	0.21300 (17)	0.0414 (6)	
O34	0.58625 (5)	1.1691 (4)	0.2537 (2)	0.0533 (8)	
Cl2	0.72028 (14)	0.0671 (7)	0.6164 (4)	0.0330 (12)	0.6667
O6	0.72004 (11)	0.1404 (8)	0.5356 (3)	0.0508 (14)	0.6667
O7	0.74955 (14)	0.0373 (12)	0.6530 (4)	0.0347 (14)	0.6667
O8	0.70409 (11)	−0.0720 (6)	0.6185 (4)	0.0594 (13)	0.6667
O9	0.71221 (14)	0.1840 (7)	0.6718 (4)	0.0653 (18)	0.6667
Cl1	0.7185 (2)	0.0605 (13)	0.6059 (8)	0.0297 (19)	0.3333
O10	0.7077 (3)	0.1569 (17)	0.5390 (9)	0.075 (3)	0.3333
O11	0.7465 (3)	0.040 (3)	0.6321 (12)	0.061 (4)	0.3333
O13	0.71045 (14)	−0.0957 (9)	0.5766 (6)	0.0345 (16)	0.3333
O12	0.7028 (2)	0.1098 (15)	0.6623 (7)	0.062 (3)	0.3333

Atomic displacement parameters (Å²)

	U^{11}	U^{22}	U^{33}	U^{12}	U^{13}	U^{23}
Cu1	0.0134 (2)	0.0240 (3)	0.0190 (3)	0.00191 (15)	0.00771 (17)	−0.00228 (17)
O2	0.0155 (10)	0.0281 (11)	0.0273 (11)	0.0012 (8)	0.0081 (8)	0.0001 (9)
O1	0.0179 (10)	0.0317 (11)	0.0217 (11)	0.0055 (8)	0.0081 (8)	−0.0015 (9)
O3	0.0188 (10)	0.0232 (11)	0.0244 (11)	0.0035 (8)	0.0116 (8)	−0.0004 (9)
O4	0.0319 (12)	0.0250 (11)	0.0287 (12)	0.0029 (9)	0.0075 (9)	0.0020 (9)
N2	0.0173 (12)	0.0187 (12)	0.0178 (13)	0.0007 (9)	0.0092 (10)	0.0011 (10)
N1	0.0174 (12)	0.0224 (12)	0.0177 (13)	−0.0008 (9)	0.0070 (10)	0.0009 (10)
N4	0.0168 (12)	0.0162 (12)	0.0230 (13)	0.0009 (9)	0.0125 (10)	0.0019 (10)
N7	0.0224 (13)	0.0245 (13)	0.0244 (14)	−0.0028 (10)	0.0091 (10)	−0.0018 (11)
N5	0.0196 (12)	0.0185 (12)	0.0212 (13)	0.0001 (9)	0.0111 (10)	0.0032 (10)
O5	0.0396 (15)	0.0463 (16)	0.0588 (18)	0.0157 (12)	0.0204 (13)	0.0135 (13)
N6	0.0282 (14)	0.0332 (15)	0.0278 (15)	0.0035 (11)	0.0152 (12)	−0.0062 (12)
C5	0.0171 (13)	0.0164 (14)	0.0177 (14)	−0.0015 (11)	0.0086 (11)	0.0019 (11)
C6	0.0164 (13)	0.0182 (14)	0.0188 (15)	−0.0014 (11)	0.0086 (11)	0.0016 (12)
C4	0.0168 (13)	0.0167 (14)	0.0206 (15)	−0.0028 (11)	0.0110 (11)	0.0036 (11)
C1	0.0210 (14)	0.0215 (15)	0.0185 (15)	−0.0017 (11)	0.0103 (12)	−0.0013 (12)
C26	0.0235 (16)	0.0230 (16)	0.0244 (17)	0.0019 (12)	0.0046 (12)	−0.0025 (13)
C3	0.0154 (13)	0.0228 (15)	0.0227 (16)	−0.0017 (11)	0.0086 (11)	0.0047 (12)
C11	0.0195 (14)	0.0162 (14)	0.0231 (16)	0.0006 (11)	0.0141 (12)	−0.0006 (12)
C23	0.0217 (15)	0.0276 (16)	0.0233 (16)	−0.0001 (12)	0.0105 (12)	−0.0010 (13)
C22	0.0253 (15)	0.0151 (14)	0.0263 (16)	0.0023 (11)	0.0154 (13)	0.0051 (12)
C7	0.0198 (14)	0.0198 (14)	0.0191 (15)	0.0005 (11)	0.0108 (12)	0.0007 (12)
C13	0.0173 (14)	0.0172 (14)	0.0310 (17)	0.0005 (11)	0.0129 (12)	0.0066 (13)
C12	0.0180 (14)	0.0164 (14)	0.0232 (16)	0.0009 (11)	0.0105 (12)	0.0038 (12)
C2	0.0213 (15)	0.0261 (16)	0.0173 (15)	−0.0061 (12)	0.0064 (12)	−0.0021 (12)
C8	0.0260 (16)	0.0299 (16)	0.0204 (16)	−0.0006 (13)	0.0105 (13)	−0.0041 (13)
C15	0.0220 (15)	0.0240 (16)	0.0236 (16)	−0.0015 (12)	0.0080 (12)	−0.0008 (12)
C10	0.0171 (14)	0.0299 (16)	0.0219 (16)	0.0008 (12)	0.0052 (12)	−0.0010 (13)
C17	0.0223 (15)	0.0200 (15)	0.0345 (18)	0.0022 (12)	0.0162 (13)	0.0059 (13)
C14	0.0191 (14)	0.0148 (14)	0.0234 (16)	0.0008 (11)	0.0119 (12)	0.0030 (12)
C9	0.0245 (15)	0.0362 (18)	0.0184 (16)	−0.0022 (13)	0.0043 (12)	−0.0046 (13)
C16	0.0164 (14)	0.0281 (17)	0.0368 (19)	0.0009 (12)	0.0063 (13)	0.0050 (14)
C21	0.0393 (18)	0.0216 (16)	0.0265 (18)	0.0007 (13)	0.0165 (14)	0.0055 (13)
C18	0.0248 (16)	0.0272 (17)	0.055 (2)	0.0093 (13)	0.0221 (16)	0.0100 (16)
C20	0.061 (2)	0.0200 (16)	0.037 (2)	0.0024 (15)	0.0318 (18)	0.0028 (14)
C19	0.049 (2)	0.0232 (17)	0.059 (3)	0.0109 (15)	0.042 (2)	0.0075 (17)
C27	0.0381 (19)	0.0350 (19)	0.044 (2)	−0.0129 (15)	0.0093 (16)	0.0012 (16)
C24	0.056 (3)	0.076 (3)	0.036 (2)	0.014 (2)	0.0115 (19)	−0.019 (2)
C28	0.0207 (17)	0.039 (2)	0.096 (3)	0.0010 (15)	0.0124 (19)	0.018 (2)
C25	0.057 (2)	0.054 (3)	0.049 (2)	0.027 (2)	0.029 (2)	−0.005 (2)
Cl3	0.0253 (4)	0.0231 (4)	0.0345 (4)	−0.0010 (3)	0.0093 (3)	0.0036 (3)
O32	0.0667 (18)	0.0310 (13)	0.0356 (15)	−0.0074 (12)	0.0161 (13)	−0.0069 (11)
O31	0.0470 (14)	0.0308 (13)	0.0329 (13)	0.0096 (10)	0.0157 (11)	0.0021 (10)
O33	0.0415 (14)	0.0339 (13)	0.0506 (16)	−0.0068 (11)	0.0132 (12)	0.0131 (12)
O34	0.0236 (13)	0.0569 (17)	0.078 (2)	−0.0019 (12)	0.0051 (12)	0.0301 (16)

Cl2	0.035 (2)	0.0304 (14)	0.0318 (15)	−0.0038 (10)	0.0015 (10)	0.0079 (10)
O6	0.058 (3)	0.061 (3)	0.031 (2)	0.020 (3)	0.003 (2)	0.013 (2)
O7	0.030 (3)	0.042 (3)	0.030 (3)	0.001 (2)	−0.0012 (19)	0.010 (2)
O8	0.0562 (19)	0.0482 (18)	0.068 (2)	−0.0204 (14)	−0.0038 (16)	0.0132 (16)
O9	0.087 (5)	0.054 (3)	0.069 (4)	0.010 (3)	0.049 (3)	0.000 (3)
Cl1	0.023 (3)	0.027 (2)	0.041 (4)	−0.0043 (18)	0.012 (3)	0.003 (2)
O10	0.108 (9)	0.052 (5)	0.063 (5)	0.023 (6)	0.013 (5)	0.026 (5)
O11	0.021 (3)	0.048 (7)	0.111 (12)	−0.004 (3)	0.006 (4)	−0.003 (8)
O13	0.019 (3)	0.030 (2)	0.052 (5)	0.000 (2)	0.000 (3)	0.001 (3)
O12	0.054 (6)	0.084 (7)	0.052 (4)	0.032 (5)	0.018 (5)	−0.005 (5)

Geometric parameters (Å, º)

Cu1—O2	1.960 (2)	C13—C14	1.477 (4)
Cu1—O1	1.958 (2)	C2—H2	0.9300
Cu1—O4	2.211 (2)	C8—H8	0.9300
Cu1—N2	2.003 (2)	C8—C9	1.367 (4)
Cu1—N1	1.997 (2)	C15—H15	0.9300
Cu1—O31	2.713 (2)	C15—C14	1.414 (4)
O2—C26	1.255 (4)	C15—C16	1.367 (4)
O1—C23	1.264 (4)	C10—H10	0.9300
O3—C11	1.375 (3)	C10—C9	1.393 (4)
O3—C13	1.355 (4)	C17—C16	1.399 (5)
O4—H4A	0.9082	C17—C18	1.425 (4)
O4—H4B	0.9052	C9—H9	0.9300
N2—C5	1.356 (4)	C16—H16	0.9300
N2—C1	1.332 (4)	C21—H21	0.9300
N1—C6	1.357 (4)	C21—C20	1.368 (5)
N1—C10	1.328 (4)	C18—H18	0.9300
N4—C13	1.303 (4)	C18—C19	1.372 (6)
N4—C12	1.386 (3)	C20—H20	0.9300
N7—C26	1.300 (4)	C20—C19	1.396 (6)
N7—C27	1.449 (4)	C19—H19	0.9300
N7—C28	1.442 (4)	C27—H27A	0.9600
N5—C22	1.372 (4)	C27—H27B	0.9600
N5—C14	1.319 (4)	C27—H27C	0.9600
O5—H5A	0.8521	C24—H24A	0.9600
O5—H5B	0.8497	C24—H24B	0.9600
N6—C23	1.298 (4)	C24—H24C	0.9600
N6—C24	1.425 (5)	C28—H28A	0.9600
N6—C25	1.451 (4)	C28—H28B	0.9600
C5—C6	1.449 (4)	C28—H28C	0.9600
C5—C4	1.404 (4)	C25—H25A	0.9600
C6—C7	1.405 (4)	C25—H25B	0.9600
C4—C3	1.406 (4)	C25—H25C	0.9600
C4—C12	1.437 (4)	Cl3—O32	1.449 (3)
C1—H1	0.9300	Cl3—O31	1.428 (2)
C1—C2	1.395 (4)	Cl3—O33	1.430 (2)

C26—H26	0.9300	Cl3—O34	1.427 (3)
C3—H3	0.9300	Cl2—O6	1.452 (6)
C3—C2	1.373 (4)	Cl2—O7	1.460 (6)
C11—C7	1.424 (4)	Cl2—O8	1.410 (7)
C11—C12	1.366 (4)	Cl2—O9	1.435 (7)
C23—H23	0.9300	Cl1—O10	1.380 (13)
C22—C17	1.421 (4)	Cl1—O11	1.358 (12)
C22—C21	1.407 (5)	Cl1—O13	1.423 (11)
C7—C8	1.405 (4)	Cl1—O12	1.365 (12)

O2—Cu1—O4	84.60 (9)	C9—C8—C7	118.8 (3)
O2—Cu1—N2	168.83 (9)	C9—C8—H8	120.6
O2—Cu1—N1	93.56 (9)	C14—C15—H15	120.9
O2—Cu1—O31	90.49 (8)	C16—C15—H15	120.9
O1—Cu1—O2	91.45 (8)	C16—C15—C14	118.2 (3)
O1—Cu1—O4	92.21 (8)	N1—C10—H10	118.9
O1—Cu1—N2	91.07 (9)	N1—C10—C9	122.2 (3)
O1—Cu1—N1	168.47 (9)	C9—C10—H10	118.9
O1—Cu1—O31	81.37 (8)	C22—C17—C18	118.3 (3)
O4—Cu1—O31	171.83 (8)	C16—C17—C22	118.2 (3)
N2—Cu1—O4	106.18 (9)	C16—C17—C18	123.5 (3)
N2—Cu1—O31	79.14 (8)	N5—C14—C13	117.1 (3)
N1—Cu1—O4	98.60 (9)	N5—C14—C15	124.6 (3)
N1—Cu1—N2	82.09 (9)	C15—C14—C13	118.3 (3)
N1—Cu1—O31	88.20 (8)	C8—C9—C10	120.1 (3)
C26—O2—Cu1	125.1 (2)	C8—C9—H9	120.0
C23—O1—Cu1	118.96 (19)	C10—C9—H9	120.0
C13—O3—C11	103.7 (2)	C15—C16—C17	119.8 (3)
Cu1—O4—H4A	112.6	C15—C16—H16	120.1
Cu1—O4—H4B	111.5	C17—C16—H16	120.1
H4A—O4—H4B	106.5	C22—C21—H21	119.6
C5—N2—Cu1	112.50 (19)	C20—C21—C22	120.7 (3)
C1—N2—Cu1	127.96 (19)	C20—C21—H21	119.6
C1—N2—C5	118.4 (2)	C17—C18—H18	119.7
C6—N1—Cu1	112.56 (18)	C19—C18—C17	120.5 (3)
C10—N1—Cu1	128.20 (19)	C19—C18—H18	119.7
C10—N1—C6	118.9 (2)	C21—C20—H20	119.7
C13—N4—C12	104.1 (2)	C21—C20—C19	120.6 (3)
C26—N7—C27	121.5 (3)	C19—C20—H20	119.7
C26—N7—C28	121.5 (3)	C18—C19—C20	120.4 (3)
C28—N7—C27	116.9 (3)	C18—C19—H19	119.8
C14—N5—C22	117.3 (3)	C20—C19—H19	119.8
H5A—O5—H5B	104.4	N7—C27—H27A	109.5
C23—N6—C24	120.7 (3)	N7—C27—H27B	109.5
C23—N6—C25	121.8 (3)	N7—C27—H27C	109.5
C24—N6—C25	117.5 (3)	H27A—C27—H27B	109.5
N2—C5—C6	115.5 (2)	H27A—C27—H27C	109.5
N2—C5—C4	122.7 (3)	H27B—C27—H27C	109.5

C4—C5—C6	121.8 (2)	N6—C24—H24A	109.5
N1—C6—C5	116.0 (2)	N6—C24—H24B	109.5
N1—C6—C7	121.9 (3)	N6—C24—H24C	109.5
C7—C6—C5	122.1 (2)	H24A—C24—H24B	109.5
C5—C4—C3	117.6 (2)	H24A—C24—H24C	109.5
C5—C4—C12	115.4 (3)	H24B—C24—H24C	109.5
C3—C4—C12	126.9 (3)	N7—C28—H28A	109.5
N2—C1—H1	118.8	N7—C28—H28B	109.5
N2—C1—C2	122.4 (3)	N7—C28—H28C	109.5
C2—C1—H1	118.8	H28A—C28—H28B	109.5
O2—C26—N7	123.6 (3)	H28A—C28—H28C	109.5
O2—C26—H26	118.2	H28B—C28—H28C	109.5
N7—C26—H26	118.2	N6—C25—H25A	109.5
C4—C3—H3	120.5	N6—C25—H25B	109.5
C2—C3—C4	119.1 (3)	N6—C25—H25C	109.5
C2—C3—H3	120.5	H25A—C25—H25B	109.5
O3—C11—C7	126.8 (3)	H25A—C25—H25C	109.5
C12—C11—O3	108.1 (2)	H25B—C25—H25C	109.5
C12—C11—C7	125.1 (2)	O31—Cl3—O32	108.18 (15)
O1—C23—N6	123.9 (3)	O31—Cl3—O33	110.89 (15)
O1—C23—H23	118.1	O33—Cl3—O32	110.35 (15)
N6—C23—H23	118.1	O34—Cl3—O32	107.92 (18)
N5—C22—C17	122.0 (3)	O34—Cl3—O31	109.61 (17)
N5—C22—C21	118.7 (3)	O34—Cl3—O33	109.82 (16)
C21—C22—C17	119.3 (3)	Cl3—O31—Cu1	133.25 (13)
C6—C7—C11	114.0 (3)	O6—Cl2—O7	106.6 (5)
C6—C7—C8	118.1 (3)	O8—Cl2—O6	117.4 (5)
C8—C7—C11	127.9 (3)	O8—Cl2—O7	110.9 (5)
O3—C13—C14	118.6 (3)	O8—Cl2—O9	109.2 (5)
N4—C13—O3	115.2 (2)	O9—Cl2—O6	109.0 (5)
N4—C13—C14	126.2 (3)	O9—Cl2—O7	102.7 (6)
N4—C12—C4	129.5 (3)	O10—Cl1—O13	103.4 (10)
C11—C12—N4	109.0 (2)	O11—Cl1—O10	122.3 (12)
C11—C12—C4	121.5 (3)	O11—Cl1—O13	101.0 (11)
C1—C2—H2	120.1	O11—Cl1—O12	118.5 (13)
C3—C2—C1	119.8 (3)	O12—Cl1—O10	100.2 (10)
C3—C2—H2	120.1	O12—Cl1—O13	110.5 (9)
C7—C8—H8	120.6		

Cu1—O2—C26—N7	−164.5 (2)	C3—C4—C12—C11	−179.0 (3)
Cu1—O1—C23—N6	166.9 (2)	C11—O3—C13—N4	0.5 (3)
Cu1—N2—C5—C6	−10.3 (3)	C11—O3—C13—C14	−178.7 (2)
Cu1—N2—C5—C4	167.4 (2)	C11—C7—C8—C9	−176.7 (3)
Cu1—N2—C1—C2	−164.2 (2)	C22—N5—C14—C13	179.0 (2)
Cu1—N1—C6—C5	6.4 (3)	C22—N5—C14—C15	0.3 (4)
Cu1—N1—C6—C7	−172.7 (2)	C22—C17—C16—C15	0.2 (4)
Cu1—N1—C10—C9	174.1 (2)	C22—C17—C18—C19	0.6 (4)
O3—C11—C7—C6	−177.9 (3)	C22—C21—C20—C19	1.3 (5)

O3—C11—C7—C8	0.7 (5)	C7—C11—C12—N4	−178.0 (3)
O3—C11—C12—N4	0.3 (3)	C7—C11—C12—C4	2.0 (4)
O3—C11—C12—C4	−179.6 (2)	C7—C8—C9—C10	0.6 (5)
O3—C13—C14—N5	0.4 (4)	C13—O3—C11—C7	177.8 (3)
O3—C13—C14—C15	179.2 (2)	C13—O3—C11—C12	−0.5 (3)
N2—C5—C6—N1	2.6 (4)	C13—N4—C12—C4	179.9 (3)
N2—C5—C6—C7	−178.3 (2)	C13—N4—C12—C11	0.0 (3)
N2—C5—C4—C3	−1.2 (4)	C12—N4—C13—O3	−0.3 (3)
N2—C5—C4—C12	−179.2 (2)	C12—N4—C13—C14	178.8 (3)
N2—C1—C2—C3	−1.1 (4)	C12—C4—C3—C2	−179.6 (3)
N1—C6—C7—C11	175.9 (2)	C12—C11—C7—C6	0.1 (4)
N1—C6—C7—C8	−2.7 (4)	C12—C11—C7—C8	178.7 (3)
N1—C10—C9—C8	−2.2 (5)	C10—N1—C6—C5	−179.6 (3)
N4—C13—C14—N5	−178.7 (3)	C10—N1—C6—C7	1.3 (4)
N4—C13—C14—C15	0.0 (4)	C17—C22—C21—C20	−0.4 (4)
N5—C22—C17—C16	−0.7 (4)	C17—C18—C19—C20	0.3 (5)
N5—C22—C17—C18	179.1 (3)	C14—N5—C22—C17	0.5 (4)
N5—C22—C21—C20	179.9 (3)	C14—N5—C22—C21	−179.8 (2)
C5—N2—C1—C2	2.6 (4)	C14—C15—C16—C17	0.5 (4)
C5—C6—C7—C11	−3.1 (4)	C16—C15—C14—N5	−0.8 (4)
C5—C6—C7—C8	178.2 (3)	C16—C15—C14—C13	−179.5 (3)
C5—C4—C3—C2	2.7 (4)	C16—C17—C18—C19	−179.6 (3)
C5—C4—C12—N4	178.9 (3)	C21—C22—C17—C16	179.6 (3)
C5—C4—C12—C11	−1.2 (4)	C21—C22—C17—C18	−0.6 (4)
C6—N1—C10—C9	1.2 (4)	C21—C20—C19—C18	−1.3 (5)
C6—C5—C4—C3	176.3 (2)	C18—C17—C16—C15	−179.7 (3)
C6—C5—C4—C12	−1.8 (4)	C27—N7—C26—O2	−179.8 (3)
C6—C7—C8—C9	1.7 (4)	C24—N6—C23—O1	0.4 (5)
C4—C5—C6—N1	−175.0 (2)	C28—N7—C26—O2	0.9 (5)
C4—C5—C6—C7	4.1 (4)	C25—N6—C23—O1	178.9 (3)
C4—C3—C2—C1	−1.6 (4)	O32—Cl3—O31—Cu1	46.4 (2)
C1—N2—C5—C6	−179.0 (2)	O33—Cl3—O31—Cu1	167.57 (17)
C1—N2—C5—C4	−1.4 (4)	O34—Cl3—O31—Cu1	−71.0 (2)
C3—C4—C12—N4	1.1 (5)		

Hydrogen-bond geometry (Å, º)

D—H···*A*	*D*—H	H···*A*	*D*···*A*	*D*—H···*A*
O4—H4*A*···O5	0.91	1.94	2.808 (3)	160
O4—H4*B*···O32^{i}	0.91	1.96	2.782 (3)	151
O5—H5*A*···O11^{ii}	0.85	2.02	2.862 (18)	170
O5—H5*B*···O10	0.85	1.95	2.790 (13)	171
O5—H5*A*···O7^{ii}	0.85	2.11	2.954 (7)	174
O5—H5*B*···O6	0.85	2.07	2.905 (7)	165

Symmetry codes: (i) *x*, *y*−1, *z*; (ii) −*x*+3/2, −*y*+1/2, −*z*+1.